The Astrophysical Journal Letters, 964:L7 (7pp), 2024 March 20 https://doi.org/10.3847/2041-8213/ad2fb3

A Relativistic Double Neutron Star Binary PSR J1846-0513

D. Zhao[1,2,3,4], N. Wang[2,3,4], J. P. Yuan[2,3,4], D. Li[5,2,6,7], P. Wang[5,8], M. Y. Xue[5], W. W. Zhu[5,8], C. C. Miao[7], W. M. Yan[2,3,4], J. B. Wang[2,3,9], J. M. Yao[2,3,4], Q. D. Wu[2,3,4], S. Q. Wang[2,3,4], S. N. Sun[2,3,4], F. F. Kou[2,3,4], Y. T. Chen[5,6], S. J. Dang[10], Y. Feng[7], Z. J. Liu[10], X. L. Miao[5], L. Q. Meng[5], M. Yuan[5], C. H. Niu[5,11], J. R. Niu[5], L. Qian[5], S. Wang[12], X. Y. Xie[10], Y. F. Xiao[13], Y. L. Yue[5], S. P. You[10], X. H. Yu[10], R. S. Zhao[10], R. Yuen[2,3,4], X. Zhou[2,3,4], L. Zhang[5], Y. B. Wang[14], J. F. Wu[14], Z. Y. Gan[14], Z. Y. Sun[14], and C. J. Wang[14]
[1] School of Physical Science and Technology, Xinjiang University, Urumqi, Xinjiang 830046, People's Republic of China
[2] Xinjiang Astronomical Observatory, Chinese Academy of Sciences, 150 Science 1-Street, Urumqi, Xinjiang 830011, People's Republic of China; na.wang@xao.ac.cn, yuanjp@xao.ac.cn
[3] Key Laboratory of Radio Astronomy, Chinese Academy of Sciences, Urumqi, Xinjiang 830011, People's Republic of China
[4] Xinjiang Key Laboratory of Radio Astrophysics, 150 Science 1-Street, Urumqi, Xinjiang 830011, People's Republic of China
[5] National Astronomical Observatories, Chinese Academy of Sciences, A20 Datun Road, Chaoyang District, Beijing 100101, People's Republic of China; dili@nao.cas.cn
[6] University of Chinese Academy of Sciences, Beijing 100049, People's Republic of China
[7] Zhejiang Lab, Hangzhou, Zhejiang 311121, People's Republic of China
[8] Institute for Frontiers in Astronomy and Astrophysics, Beijing Normal University, Beijing 102206, People's Republic of China
[9] Institute of Optoelectronic Technology, Lishui University, Lishui 323000, People's Republic of China
[10] Guizhou Normal University, Guiyang 550001, People's Republic of China
[11] Institute of Astrophysics, Central China Normal University, Wuhan 430079, People's Republic of China
[12] School of Computer Science, Fudan University, Shanghai 200438, People's Republic of China
[13] GuiZhou University, Guizhou 550025, People's Republic of China
[14] Tencent Youtu Lab, Shanghai 201103, People's Republic of China
Received 2023 December 27; revised 2024 February 29; accepted 2024 March 3; published 2024 March 13

Abstract

We report the timing analysis of PSR J1846−0513, a pulsar discovered by the Five-hundred-meter Aperture Spherical radio Telescope (FAST) in Commensal Radio Astronomy FAST Survey. The pulsar possesses a spin period of 23.36 ms and a spin-down rate ($\dot{P}$) of $1.0106(3) \times 10^{-18}$ s s^{-1}, and it is located in an eccentric orbit ($e \sim 0.208$) with an orbital period of 0.61 days. The characteristic age and surface magnetic field of the pulsar are found to be 366.62 Myr and 4.9178×10^{9} G, respectively, indicating that it is a recycled pulsar. Using over two years of timing data, we measure the periastron advance $\dot{\omega} = 0.8956(8)$ deg yr^{-1}. By assuming that this effect is purely relativistic, we have estimated the total mass $M = 2.6287(35) M_{\odot}$ and obtained an upper limit for the pulsar mass and a lower limit for the companion's mass. Our results indicate that this is a double neutron star system.

Unified Astronomy Thesaurus concepts: Binary pulsars (153); Pulsars (1306)

1. Introduction

Since the discovery of the first double neutron star (DNS; PSR B1913+16) by Hulse & Taylor (1975), a total of 30 DNS systems have been discovered so far, with 20 of them confirmed and 10 classified as potential candidates. Although the number of DNS systems is increasing, they only account for 0.85% of the total number of pulsars. Among these, the double pulsar system stands out as a unique example where both neutron stars (NSs) can be detected as radio pulsars. The only known double pulsar system, PSR J0737−3039A/B, was discovered by Burgay et al. (2003) and Lyne et al. (2004).

DNS systems originate from two high-mass stars. The more massive star undergoes a supernova explosion, resulting in an NS, while the other high-mass companion star remains, forming a binary system. Subsequently, before the companion star undergoes a supernova explosion, the NS accretes mass and angular momentum from the companion star, causing the rotation of the NS to accelerate to a few tens of milliseconds (Chattopadhyay et al. 2020). This process is known as the "recycling" process, and it is accompanied with X-ray radiation (Bhattacharya & van den Heuvel 1991).

Unlike systems with less-massive companion stars, pulsars in DNS systems tend to have longer rotational periods (16–186 ms). The rotational period is determined by the initial mass of the companion star, such that the smaller the initial mass of the companion star, the more efficient the accretion process becomes. If the system is fortunate enough to avoid destruction during the second supernova explosion, a DNS system will be formed.

DNS systems play an important role in various aspects of astrophysics and fundamental physics. For example, they can be used to measure relativistic effects for testing gravitational theories (Fonseca et al. 2014; Weisberg & Huang 2016; Kramer et al. 2021). They also provide insights into the formation process of millisecond pulsars (MSPs; Lewin & van der Klis 2006). DNS systems are crucial for precise mass measurements of NSs, which can help constrain the equation of state for high-density nuclear matter (Özel & Freire 2016).

The Commensal Radio Astronomy FAST survey (CRAFTS) pulsar search observations are conducted in the drift-scan mode, in which the telescope is held fixed at the meridian while the sky drifts past the telescope beams. This increases the position uncertainty in the newly discovered pulsars (especially for single-pulse detection). With the rapid growth of pulsar

candidates, we strive to swiftly follow up FAST discoveries through FAST and international collaborations (Cameron et al. 2020; Cruces et al. 2021; Miao et al. 2023). Combining all pulsars discovered in the ongoing CRAFTS and the early FAST commission pilot survey, CRAFTS has confirmed the discovery of 188 new pulsars to date.[15] This includes 40 MSPs (Wang et al. 2021; Wu et al. 2023b; Miao et al. 2023), two DNS systems (Wu et al. 2023a and this work), one high-energy young pulsar with a γ-ray counterpart (Wang et al. 2021), >20 binaries (Cruces et al. 2021; Miao et al. 2023), and >30 rotating radio transients (Chen et al. 2022).

In this paper, we report the discovery and timing solution of PSR J1846−0513. The pulsar has a spin period of 23.36 ms, and it is located in an eccentric orbit ($e \sim 0.208$) with an orbital period of 0.61 days. We propose that the pulsar is part of a mildly recycled DNS system.

Section 2 describes the details of the observational setting and data reduction procedures. In Section 3, we present the results of the timing solution. We discuss our results in Section 4.

2. Observations and Data Reduction

PSR J1846−0513 was discovered by the NAOC-Tencent collaboration through CRAFTS program (Li et al. 2018). The NAOC-Tencent collaboration designs an artificial intelligence (AI) based data processing workflow. During the "AI discrimination" process, time-phase and frequency-phase diagrams are first subjected to a shared-weight attention mechanism (Wu et al. 2023) that focuses on the phase where the pulsar signal occurs. Since positive samples of positive pulsar data are very rare, we enhance the model's discrimination ability toward rare positive pulsar samples through contrastive learning in a self-supervised manner (Tu et al. 2023). Lastly, to address the data distribution shift issue, we design and appoint decision boundaries (Xie et al. 2022) to select samples with high information value from the new domain data, followed by merging them into the previous data set for model retraining. This reduces the distribution difference between the two domains, and enhances the generalization ability of the model in the target domain. The follow-up observations were conducted using the 19-beam receiver of the FAST (Nan et al. 2011). The receiver has an effective bandwidth of 400 MHz, covering the frequency range from 1050 to 1450 MHz (Jiang et al. 2020). So far, a total of 32 observation sessions have been carried out, each lasting for 4 minutes. Polarization calibration was made by injecting diode noise with a cycle of 0.1006632960 s, which lasts for 40 s, while the telescope was directed toward a sky region offset by 10′ from the source.

We used the DSPSR[16] (van Straten & Bailes 2011) software to dedisperse and fold the pulses, and the integrated profiles for each observation has 512 phase bins. Radio frequency interference was eliminated using the PAZ and PAZI tools in the PSRCHIVE[17] software package (Hotan et al. 2004). After polarization calibration, the RMFIT tool was used to search for the Faraday rotation, based on which all observations was added and the polarization profile was plotted. The result is shown in Figure 1. We used the PSRADD tool to add all observations. Then the PAAS tool was used to generate the standard profile, and the pulse arrival times (TOAs) were obtained using the default algorithm (FFTFIT; Taylor 1992) in the PAT tool. The distance to the pulsar is estimated using the YMW16 model (Yao et al. 2017) and the NE2001 model (Cordes & Lazio 2002) for the Galactic distribution of free electrons.

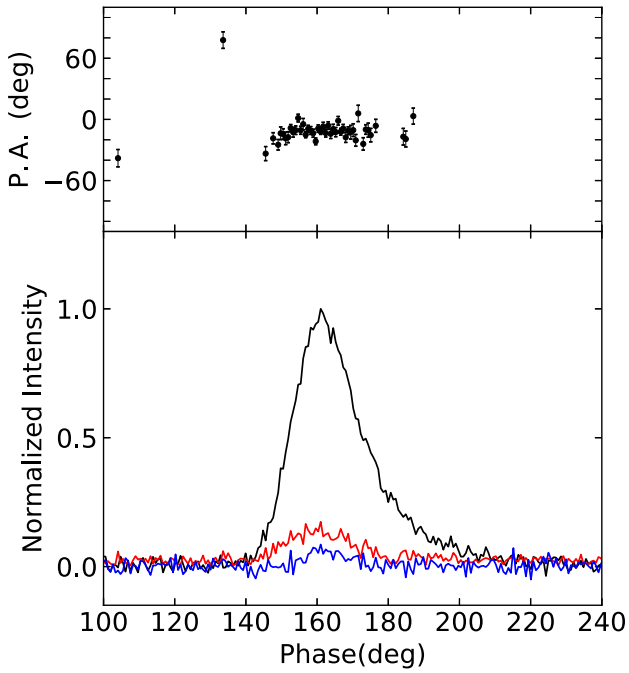

Figure 1. Polarization profiles for pulsar J1846−0513. The black, red, and blue lines in the lower panel represent the total intensity, linearly polarized intensity, and circularly polarized intensity, respectively. All profiles have been normalized by the peak intensity of the average pulse profile. The black dots with error bars in the upper panel indicate the position angle (PA) of the linearly polarized emission.

TEMPO (Nice et al. 2015) and TEMPO2 (Hobbs et al. 2006) were applied to build a phase-connected timing solution. Since PSR J1846−0513 is a newly discovered pulsar, we first used the pulsar search software PRESTO[18] (Ransom 2011) to determine an initial spin period (P) and dispersion measure (DM). Based on the initial search results, the spin period of PSR J1846−0513 changes on different epochs, indicating that it is in a binary system. We then fitted for the Keplerian parameters using a Javascript NEWFITORBIT[19] and obtained the preliminary timing solution, which was then used as the preliminary ephemeris in DRACULA[20] (Freire & Ridolfi 2018) iteration to obtain the phase-connected timing solution. Furthermore, the entire frequency was divided into two subbands, each with a different central frequency but the same bandwidth. Fitting these subbands yielded the DM value of this pulsar.

3. Results

With a data span of 2.449 yr and using the method described in Section 2, we obtained the timing solution shown in Table 1. Since the majority of the observed data are concentrated between MJD 59877.4 and MJD 60321.1, we have chosen the

[15] http://crafts.bao.ac.cn/pulsar
[16] http://dspsr.sourceforge.net/
[17] http://psrchive.sourceforge.net/
[18] https://github.com/scottransom/presto
[19] https://github.com/SixByNine/newfitorbit
[20] https://github.com/pfreire163/Dracula

Table 1
Timing Solution for PSR J1846−0513

Pulsar name	PSR J1846−0513
Measured Parameters	
R.A., α (hh:mm:ss)	18:46:09.03620(6)
decl., δ (dd:mm:ss)	−05:13:20.614(2)
Pulse frequency, ν (s^{-1})	42.79074514720(2)
First derivative of pulse frequency, $\dot{\nu}$ (s^{-2})	$-1.8505(6)\times10^{-15}$
Dispersion measure, DM (pc cm^{-3})	310.73(1)
Faraday rotation measure, RM (rad m^{-2})	−236(19)
Orbital period, P_b (days)	0.613021448(2)
Epoch of periastron, T_0 (MJD)	60004.6886971(6)
Projected semimajor axis of orbit, x (lt-s)	4.756469(21)
Longitude of periastron, ω (deg)	328.8395(3)
Orbital eccentricity, e	0.2085888(9)
Periastron advance, $\dot{\omega}$ (deg yr^{-1})	0.8956(8)
Binary model	DD
Fitting Parameters	
First TOA (MJD)	59426.6
Last TOA (MJD)	60321.2
Timing epoch (MJD)	60099.3
Data span (yr)	2.449
Number of TOAs	32
solar system ephemeris model	DE438
rms timing residual (μs)	5.518
TOA weighted factor, EFAC	1.0
Derived Parameters	
P (s)	0.023369539290791(1)
$\dot{P}$ ($s\ s^{-1}$)	$1.0106(3)\times10^{-18}$
Galactic longitude, l (deg)	27.682
Galactic latitude, b (deg)	−1.207
DM distance, d (kpc)	
NE2001	5.798
YMW16	5.1653
$\log_{10}$(Characteristic age, yr)	8.56
$\log_{10}$(Surface magnetic field strength, G)	9.69
$\log_{10}$(Edot, erg s^{-1})	33.50
Mass function, $M_\odot$	0.30745785(41)
Minimum companion mass, $m_{c,min}(M_\odot)$	1.2845
Median companion mass, $m_{c,med}(M_\odot)$	1.6048
S_{1250}(mJy)	0.096(11)

Note. The flux density at 1.25 GHz was estimated using the radiometer equation from Lorimer & Kramer (2004).

point halfway of this duration as the epoch of spin parameters and astrometric parameters. To ensure the TOA residuals χ^2 are ∼1, we have scaled the uncertainties of the TOAs using a factor called EFAC. The resulting ephemeris is ground on the JPL DE438[21] solar system ephemeris and Damour & Deruelle's (DD) binary model (Damour & Deruelle 1985, 1986) in barycentric coordinate time units, which provides a good description for eccentric binary orbits. The postfit timing residual versus MJD and orbital phase, respectively, are shown in Figure 2. The rms timing residual over 2.449 yr observation is 5.518 μs.

3.1. Pulsar Timing

From our ephemeris, we obtained a spin period of 23.36 ms, the characteristic age of 366.16 Myr, and the surface magnetic field of 4.92×10^9 G for PSR J1846−0513, indicating that the pulsar was recycled. In addition, the orbital period of this pulsar is 0.61 day, and the projected semimajor axis of the orbit is 4.75 lt-s. We obtained the mass function by

$$f(m_p, m_c) = \frac{(m_c \sin i)^3}{M^2} = \frac{4\pi^2 x^3}{T_\odot P_b^2} = 0.30745785(41) M_\odot, \quad (1)$$

where $T_\odot = GM_\odot/c^3 = 4.925490947\ \mu$s is the mass of the Sun times Newton's gravitational constant. Here, c is the speed of light and $M = m_p + m_c$ is the total mass of the system, where m_p and m_c are pulsar and companion masses, respectively. The orbit eccentricity (e ∼0.208) of this system is relatively large, which allows us to measure a post-Keplerian (PK) parameter, namely the periastron advance ($\dot{\omega}$). Assuming that this is purely relativistic, it allows the total mass of the system to be estimated combining other Kepler parameters, as shown in the following equation (Taylor & Weisberg 1982):

$$\dot{\omega} = 3\left(\frac{P_b}{2\pi}\right)^{-5/3} (T_\odot M)^{2/3} (1 - e^2)^{-1}. \quad (2)$$

We obtained $\dot{\omega} = 0.8956(8)$ deg yr^{-1} and the total mass of the system $M = 2.6287 \pm 0.0035 M_\odot$. This is very similar to the average total mass of all known DNS systems, which is $2.635(18) M_\odot$. The total mass of our system is similar with PSRs J0737−3039A (Kramer et al. 2006), B1534 + 12 (Fonseca et al. 2014), J1759 + 5036 (Agazie et al. 2021), and J1829 + 2456 (Champion et al. 2005).

We obtained the lower mass limit of m_c by combining the system total mass and the Keplerian mass function based on $\sin i = 1 (i = 90°)$:

$$m_c \geqslant \sqrt[3]{f(m_p, m_c) M^2} = 1.2856(11) M_\odot. \quad (3)$$

Due to the lack of measurement of other PK parameters, we can only impose limits on the mass for the pulsar and its companion based on $\dot{\omega}$. Figure 3 presents the correlation of m_p and m_c. We obtained an upper limit of $m_p \leqslant 1.3455 M_\odot$ for the pulsar mass and the lower limit of $m_c \geqslant 1.2845 M_\odot$ (1σ error) for the companion mass. The maximum mass of PSR J1846−0513 and the minimum mass of its companion are relatively close to the pulsar mass ($1.338 M_\odot$) and companion star mass ($1.248 M_\odot$) of PSR J0737−3039A (Kramer et al. 2006).

3.2. Origin of the System

Figure 4 shows the m_p–m_c diagram for all DNS and NS–white dwarf (WD) systems with pulsar and companion mass. It can be seen that, if the inclination angle is $i = 90°$, the mass distribution of the PSR J1846−0513 and its companion is consistent with other DNS systems. However, if the inclination angle is $i = 60°$, the mass of the pulsar reduces to $1.1443(22) M_\odot$, making it the lowest in the pulsar mass in all the known DNS systems. In addition, the mass of the companion becomes the largest at $1.4844(13) M_\odot$, which is close to $1.46(8) M_\odot$ for the companion mass of the highly eccentric PSR J0509 + 3801 (Lynch et al. 2018).

From Figure 4, we see that there are three NS-WD systems (PSRs J1528−3146, J2222−0137, and B2303+46) that are relatively consistent with PSR J1846−0513. For comparison, we list several parameters of these three NS-WD systems together with that from PSR J1846−0513 in Table 2. All PSRs J1528−3146, J2222−0137, and J1846−0513 have a larger

[21] ftp://ssd.jpl.nasa.gov/pub/eph/planets/bsp/de438.bsp

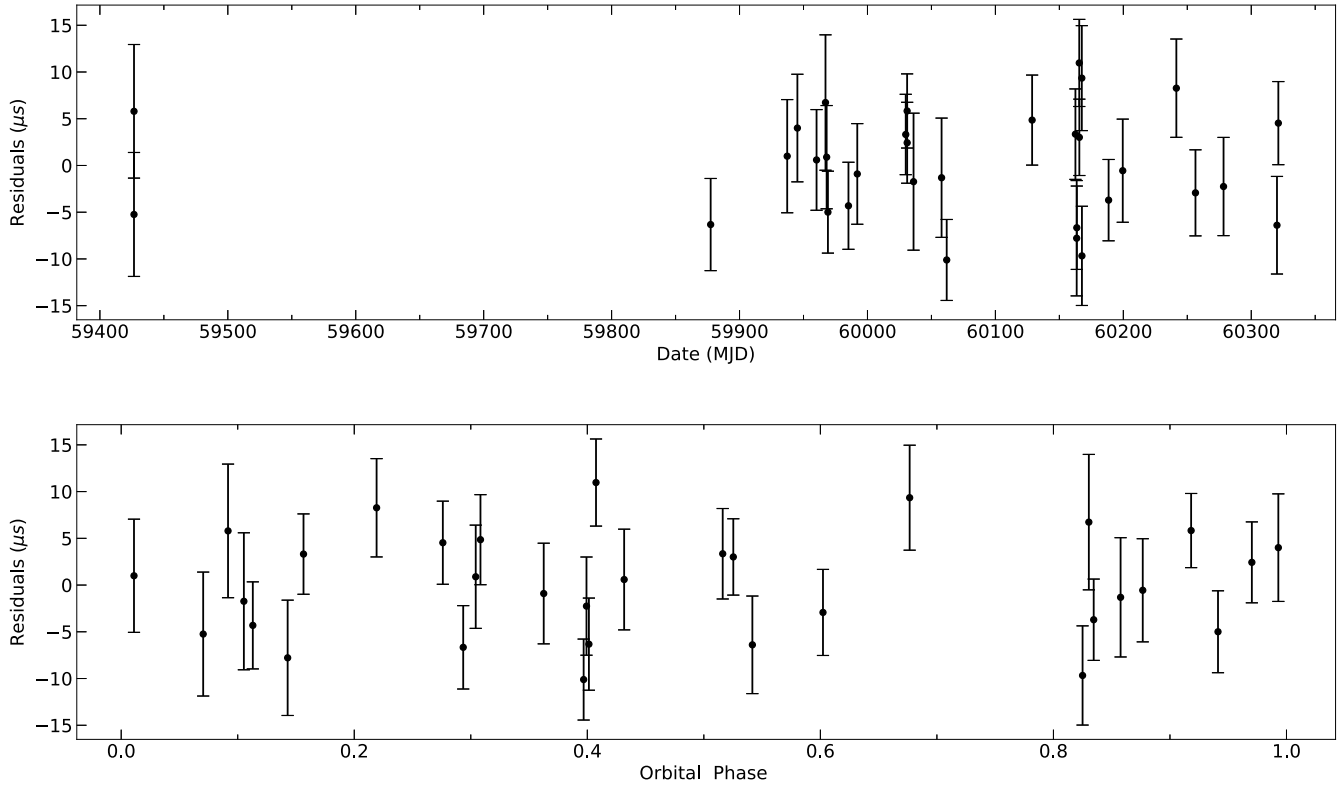

Figure 2. The best postfit timing residuals of PSR J1846−0513. The top and bottom panels show plots for MJD and orbital phase vs. postfit residuals, respectively.

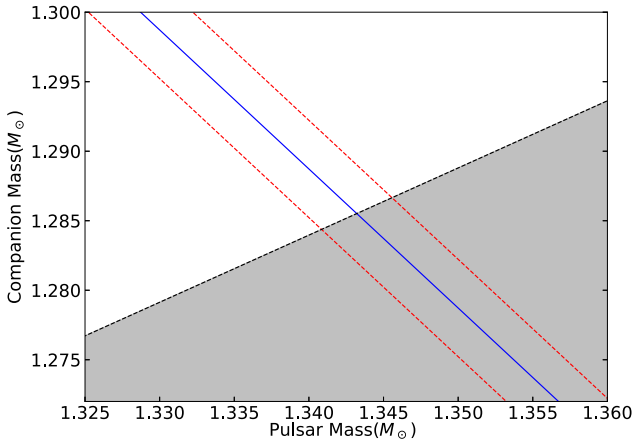

Figure 3. The m_p–m_c diagram. The blue solid line represents the measured $\dot{\omega} = 0.8956(8)$, and the red dashed line represents the measurement error of $\dot{\omega}$. The gray area is excluded due to $\sin \leqslant 1$.

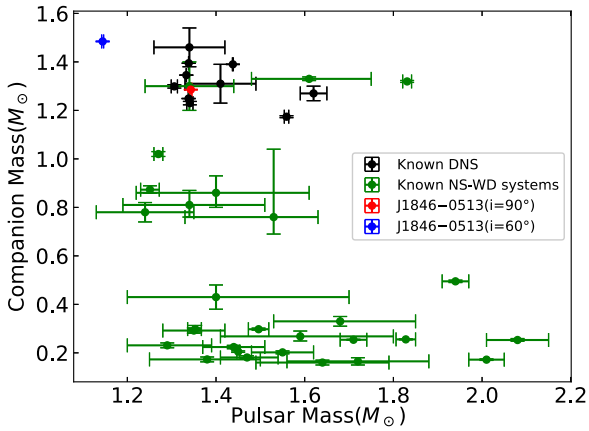

Figure 4. Mass–mass diagram of known DNS, NS-WD systems, and PSR J1846−0513. The red and blue dots represent the masses of the PSR J1846−0513 and its companion, respectively, at inclination angles of $i = 90°$ and $i = 60°$. The systems in the globular cluster are not considered in the plot.

characteristic age and smaller spin period, indicating that they have undergone recycling. However, PSR J1846−0513 is different in that it has a larger eccentricity, suggesting that the system has experienced a second supernova explosion. PSR B2303 + 46 has not undergone recycling, and it was born after the WD (van Kerkwijk & Kulkarni 1999; Davies et al. 2002). It suggests that PSR J1846−0513 is completely different from PSR B2303 + 46. Therefore, we believe that PSR 1846−0513 belongs to a DNS system.

We calculated the system mass ratios ($q = m_p/m_c$) for inclination angles of 90° and 60°, and the results are 1.04 and 0.76, respectively, which are consistent with the mass ratios ∼1 typically observed in DNS systems. Tauris et al. (2017) suggests that there is a correlation between P_b and P of the recycled pulsars in the DNS systems, which is given by

$$P \approx 44 \text{ ms}(P_b/\text{days})^{0.26}. \quad (4)$$

In Figure 5(a), we plotted the relationship between P_b and P for the currently known recycled DNS systems, with the red star standing for PSR J1846−0513. The figure shows that the spin period of recycled pulsars in DNS systems increases with the orbital period. It also shows that PSR J1846−0513 remains consistent with Equation (4), indicating that this pulsar has been recycled. In shorter orbits, the companion star is likely to transfer more material and angular momentum to the NS. The transfer of angular momentum from the companion star to the NS leads to an increase in the rotation speed of the latter,

Table 2
The Spin Period, Orbital Period, Surface Magnetic Field, Characteristic Age, and Eccentricity of Three NS-WD Systems and PSR J1846−0513

PSR	P (ms)	P_b (days)	B_{surf} (G)	τ_c (yr)	e
J1528−3146	60.82	3.18	3.94×10^9	3.87×10^9	0.000213
J2222−0137	32.81	2.44	4.42×10^9	8.96×10^8	0.000380926
B2303 + 46	1066.37	12.33	7.88×10^{11}	2.97×10^7	0.658369
J1846−0513	23.36	0.61	4.92×10^9	3.66×10^8	0.2085888

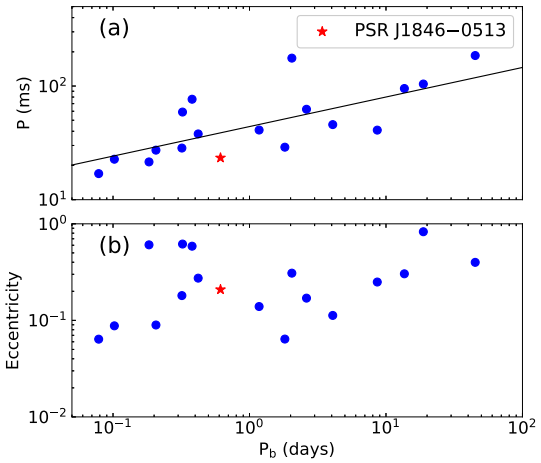

Figure 5. Panel (a): the black solid line is obtained from Equation (4). The blue points represent the relationship between the spin period and orbital period of recycled pulsars in known DNS systems. Panel (b): plot for orbital eccentricity as a function of orbital period for the recycled DNS systems. The red star represents PSR J1846−0513. DNS systems in globular clusters are not considered in our sample, because the complex situation in globular clusters may lead to inaccuracy in the eccentricity near the other stars in these systems.

resulting in a shorter rotation period. Therefore, shorter orbits are often associated with faster rotating pulsars.

Similarly, the eccentricity and orbital period of DNS systems are expected to be correlated. This is because systems with longer orbital periods experience less mass transfer, allowing the second NS to retain higher mass during its explosion and leading to larger system eccentricities. Although the correlation between eccentricity and orbital period may appear weak in Figure 5(b), it shows that PSR J1846−0513 belongs to the subpopulation of short orbital period ($P_b < 1$ day; Andrews & Mandel 2019), where their low eccentricities are generated by a combination of two types of kicks. The first type is the birth kick imparted during the collapse of the progenitor NS, and systems with small birth kicks result in low eccentricity. The second type, known as the "Blaauw" kick (Blaauw 1961), is caused by instantaneous mass loss. The mass loss is symmetric in the frame of the collapsing object but asymmetric in the center-of-mass frame of the binary system. The eccentricity is determined solely by the ratio of the mass lost during the supernova event to the mass remaining in the binary system, with higher ratios resulting in higher eccentricities.

According to Tauris et al. (2013, 2015), systems that experienced small Blaauw kicks ought to also undergo small natal kicks. Research indicates that small asymmetric kicks occurred in certain systems (Wex et al. 2000; Willems et al. 2004; Stairs et al. 2006), such as the double pulsar system (PSR J0737−3039A/B; Tauris et al. 2015, 2017). This phenomenon mainly occurs in electron-capture supernovae (see Tauris et al. 2017). Such supernovae produce small natal and Blaauw kicks, consistent with short orbital period and the formation of lower-mass second NSs. The slightly higher mass of the companion star in such scenarios might be due to additional fallback material during the supernova event (Fryer & Kalogera 2001; Fryer 2009).

We checked the optical and high-energy archival data[22] and no WD counterpart is found for PSR J1846−0513. Based on the DM value of PSR J1846−0513, we conducted an accelerated search with zmax of 200 using PRESTO (see footnote 19) (Ransom 2011) on the beam that detected the pulsar signal. Unfortunately, we did not detect another periodic radio signal. If the companion is or was a pulsar, its nondetection may indicate that it is a dim source, or it has ceased emitting radio radiation, or that its radio beam does not sweep across our line of sight (Lorimer et al. 2006; Lazarus et al. 2016).

4. Discussion

In this paper we report the discovery of PSR J1846−0513 and its timing analysis. It is a recycled pulsar with a spin period of 23.36 ms, and it is located in an eccentric orbit ($e \sim 0.208$) with an orbital period of 0.61 days. Due to its significant periastron advance, we were able to accurately measure the periastron advance ($\dot{\omega} = 0.8956(8)$ deg yr^{-1}). Through this measurement, we derived the total mass of the system $M = 2.6287(35) M_\odot$ and estimated the upper limit of m_p and the lower limit of m_c. The mass ratio of the system is consistent with the distributions of spin period and orbital period of recycled pulsars in known DNS systems. The relationship between orbital period and eccentricity also conforms to the recycled pulsars in known DNS systems. Combining with the mass of this system, we conclude that PSR J1846−0513 is a DNS system.

If two or more PK parameters can be measured, an accurate system mass will be obtained, while more than two PK parameters can be used to test general relativity. Regarding other PK parameters, e.g., Einstein delay (γ), they can be measured for a system with a significant advance of periastron. For $m_p = m_c = 1.31 M_\odot$, we expect an Einstein delay of $\gamma = 1.75$ ms. Simulations indicate that continuous timing will allow γ to be measured in approximately 4 yr. At present, we did not detect Shapiro delay in this system, which may be due to fewer observations and a short data set that could not cover the majority of the orbital phase. Freire & Wex (2010) proposed two new PK parameters, namely h_3 and ς, which are the "orthometric amplitude" and "orthometric ratio" parameters of the Shapiro delay, respectively. They suggest that these are superior in describing the Shapiro delay, with the following

[22] Available at https://simbad.u-strasbg.fr/simbad/.

equation:

$$h_3 = r\varsigma^3 = T_{\odot} m_c \left(\frac{\sin i}{1 + |\cos i|} \right)^3, \quad (5)$$

where r is "range" of Shapiro delay. For the inclination angles of 60° and 90°, the values of h_3 are 1.407(1) and 6.332(6) μs, respectively. From these values, if the orbit inclination angle is high enough, it may be possible to continue observing the system in the future so that the Shapiro delay can be detected and directly measure the quality of this system. Although the radio emission from the second NS has not been detected at present, if the second NS is still active as a radio pulsar, it is hoped that its radio emission can be observed in the future considering its advance of periastron, even though this may take a long time.

At present, CRAFTS has discovered approximately 234 pulsar candidates, of which more than 20 are in binary systems. Currently, there are currently approximately two possible DNS systems discovered. Based on the observations of 1364 normal pulsars and 43 MSPs in the Parkes Multibeam Pulsar Survey (Camilo et al. 2000), Parkes High-latitude Multibeam Pulsar Survey (Burgay et al. 2006), and Parkes Swinburne Multibeam Pulsar Survey (Edwards et al. 2001), we utilized the PsrPopPy[23] software (Bates et al. 2014), and the Monte Carlo method to simulate the number for isolated normal pulsars and isolated MSPs in the Galaxy, and we obtained 134,734 and 31,189, respectively. Using this sample, CRAFTS is simulated for the sky area of decl. between −14° and 65° with an effective integration time of 15 s. The results shows that 2431 normal pulsars and 331 MSPs can be found. Currently, it is found that the DNS systems only account for 0.85% of the total number of pulsars. It is expected that approximately 21 DNS systems may be discovered by CRAFTS in the future.

Acknowledgments

This work is supported by the National Key Research and Development Program of China (No. 2022YFC2205203), the National Natural Science Foundation of China grants (Nos. 12288102, 12041303, 12041304, 12273100, 11988101, T2241020), and the Major Science and Technology Program of Xinjiang Uygur Autonomous Region (Nos. 2022A03013-3, 2022A03013-4). D.L. is a New Cornerstone investigator, and is supported by the 2020 project of Xinjiang Uygur autonomous region of China for flexibly fetching in upscale talents. P.W. acknowledges support from the National Natural Science Foundation of China under grant U2031117, the Youth Innovation Promotion Association CAS (id. 2021055), and the Cultivation Project for FAST Scientific Payoff and Research Achievement of CAMS-CAS. W.W.Z. is supported by the National SKA Program of China No. 2020SKA0120200, and National Nature Science Foundation grant No. 11873067. S.J.D. is supported by Guizhou Provincial Science and Technology Foundation (Nos. ZK[2022]304), the Major Science and Technology Program of Xinjiang Uygur Autonomous Region (No. 2022A03013-4), and the Scientific Research Project of the Guizhou Provincial Education (Nos. KY[2022]132). J.M.Y. is sponsored by the Natural Science Foundation of Xinjiang Uygur Autonomous Region (No. 2022D01D85). This work utilized data from FAST (Five-hundred-meter Aperture Spherical radio Telescope). FAST is a Chinese national megascience facility, operated by the National Astronomical Observatories, Chinese Academy of Sciences. We would like to thank the FAST CRAFTS group and XAO pulsar group for data provided and helpful suggestions that led to significant improvements in our study. R.Y. is supported by the National SKA Program of China No. 2020SKA0120200, the National Key Program for Science and Technology Research and Development No. 2022YFC2205201, and the Major Science and Technology Program of Xinjiang Uygur Autonomous Region No. 2022A03013-2. This research is partly supported by the Operation, Maintenance and Upgrading Fund for Astronomical Telescopes and Facility Instruments, budgeted by the Ministry of Finance of China (MOF) and administered by the CAS.

[23] http://github.com/samb8s/PsrPopPy

ORCID iDs

D. Zhao https://orcid.org/0009-0007-8062-1454
N. Wang https://orcid.org/0000-0002-9786-8548
J. P. Yuan https://orcid.org/0000-0002-5381-6498
D. Li https://orcid.org/0000-0003-3010-7661
P. Wang https://orcid.org/0000-0002-3386-7159
M. Y. Xue https://orcid.org/0000-0001-8018-1830
W. W. Zhu https://orcid.org/0000-0001-5105-4058
C. C. Miao https://orcid.org/0000-0002-9441-2190
W. M. Yan https://orcid.org/0000-0002-7662-3875
J. B. Wang https://orcid.org/0000-0001-9782-1603
J. M. Yao https://orcid.org/0000-0002-4997-045X
S. Q. Wang https://orcid.org/0000-0003-4498-6070
F. F. Kou https://orcid.org/0000-0002-0069-831X
Y. Feng https://orcid.org/0000-0002-0475-7479
L. Q. Meng https://orcid.org/0000-0002-2885-568X
M. Yuan https://orcid.org/0000-0003-1874-0800
C. H. Niu https://orcid.org/0000-0001-6651-7799
J. R. Niu https://orcid.org/0000-0001-8065-4191
L. Qian https://orcid.org/0000-0003-0597-0957
S. Wang https://orcid.org/0000-0002-1570-7485
Y. L. Yue https://orcid.org/0000-0003-4415-2148
X. Zhou https://orcid.org/0000-0003-4686-5977
L. Zhang https://orcid.org/0000-0001-8539-4237
Z. Y. Gan https://orcid.org/0000-0002-2431-1159
C. J. Wang https://orcid.org/0000-0003-4216-8090

References

Agazie, G. Y., Mingyar, M. G., McLaughlin, M. A., et al. 2021, ApJ, 922, 35
Andrews, J. J., & Mandel, I. 2019, ApJL, 880, L8
Bates, S. D., Lorimer, D. R., Rane, A., & Swiggum, J. 2014, MNRAS, 439, 2893
Bhattacharya, D., & van den Heuvel, E. P. J. 1991, PhR, 203, 1
Blaauw, A. 1961, BAN, 15, 265
Burgay, M., D'Amico, N., Possenti, A., et al. 2003, Natur, 426, 531
Burgay, M., Joshi, B. C., D'Amico, N., et al. 2006, MNRAS, 368, 283
Cameron, A. D., Li, D., Hobbs, G., et al. 2020, MNRAS, 495, 3515
Camilo, F., Lyne, A. G., Manchester, R. N., et al. 2000, in ASP Conf. Ser. 202, IAU Colloq. 177: Pulsar Astronomy—2000 and Beyond, ed. M. Kramer, N. Wex, & R. Wielebinski (San Francisco, CA: ASP), 3
Champion, D. J., Lorimer, D. R., McLaughlin, M. A., et al. 2005, MNRAS, 363, 929
Chattopadhyay, D., Stevenson, S., Hurley, J. R., Rossi, L. J., & Flynn, C. 2020, MNRAS, 494, 1587
Chen, J. L., Wen, Z. G., Yuan, J. P., et al. 2022, ApJ, 934, 24
Cordes, J. M., & Lazio, T. J. W. 2002, arXiv:astro-ph/0207156
Cruces, M., Champion, D. J., Li, D., et al. 2021, MNRAS, 508, 300
Damour, T., & Deruelle, N. 1985, AIHPA, 43, 107
Damour, T., & Deruelle, N. 1986, AIHPA, 44, 263
Davies, M. B., Ritter, H., & King, A. 2002, MNRAS, 335, 369

Edwards, R. T., Bailes, M., van Straten, W., & Britton, M. C. 2001, MNRAS, 326, 358
Fonseca, E., Stairs, I. H., & Thorsett, S. E. 2014, ApJ, 787, 82
Freire, P. C. C., & Ridolfi, A. 2018, MNRAS, 476, 4794
Freire, P. C. C., & Wex, N. 2010, MNRAS, 409, 199
Fryer, C. L. 2009, ApJ, 699, 409
Fryer, C. L., & Kalogera, V. 2001, ApJ, 554, 548
Hobbs, G. B., Edwards, R. T., & Manchester, R. N. 2006, MNRAS, 369, 655
Hotan, A. W., van Straten, W., & Manchester, R. N. 2004, PASA, 21, 302
Hulse, R. A., & Taylor, J. H. 1975, ApJL, 195, L51
Jiang, P., Tang, N.-Y., Hou, L.-G., et al. 2020, RAA, 20, 064
Kramer, M., Stairs, I. H., Manchester, R. N., et al. 2006, Sci, 314, 97
Kramer, M., Stairs, I. H., Manchester, R. N., et al. 2021, PhRvX, 11, 041050
Lazarus, P., Freire, P. C. C., Allen, B., et al. 2016, ApJ, 831, 150
Lewin, W. H. G., & van der Klis, M. 2006, Compact Stellar X-ray Sources (Cambridge: Cambridge Univ. Press), 39
Li, D., Wang, P., Qian, L., et al. 2018, IMMag, 19, 112
Lorimer, D. R., & Kramer, M. 2004, Handbook of Pulsar Astronomy .4 (Cambridge: Cambridge Univ. Press)
Lorimer, D. R., Stairs, I. H., Freire, P. C., et al. 2006, ApJ, 640, 428
Lynch, R. S., Swiggum, J. K., Kondratiev, V. I., et al. 2018, ApJ, 859, 93
Lyne, A. G., Burgay, M., Kramer, M., et al. 2004, Sci, 303, 1153
Miao, C. C., Zhu, W. W., Li, D., et al. 2023, MNRAS, 518, 1672
Nan, R., Li, D., Jin, C., et al. 2011, IJMPD, 20, 989
Nice, D., Demorest, P., Stairs, I., et al. 2015, Tempo: Pulsar timing data analysis, Astrophysics Source Code Library, ascl:1509.002
Özel, F., & Freire, P. 2016, ARA&A, 54, 401
Ransom, S. 2011, PRESTO: PulsaR Exploration and Search TOolkit, Astrophysics Source Code Library, ascl:1107.017
Stairs, I. H., Thorsett, S. E., Dewey, R. J., Kramer, M., & McPhee, C. A. 2006, MNRAS, 373, L50
Tauris, T. M., Kramer, M., Freire, P. C. C., et al. 2017, ApJ, 846, 170
Tauris, T. M., Langer, N., Moriya, T. J., et al. 2013, ApJL, 778, L23
Tauris, T. M., Langer, N., & Podsiadlowski, P. 2015, MNRAS, 451, 2123
Taylor, J. H. 1992, RSPTA, 341, 117
Taylor, J. H., & Weisberg, J. M. 1982, ApJ, 253, 908
Tu, Y., Zhang, B., Li, Y., et al. 2023, in Proc.of the IEEE/CVF Conf. on Computer Vision and Pattern Recognition, 16186
van Kerkwijk, M. H., & Kulkarni, S. R. 1999, ApJL, 516, L25
van Straten, W., & Bailes, M. 2011, PASA, 28, 1
Wang, P., Li, D., Clark, C. J., et al. 2021, SCPMA, 64, 129562
Weisberg, J. M., & Huang, Y. 2016, ApJ, 829, 55
Wex, N., Kalogera, V., & Kramer, M. 2000, ApJ, 528, 401
Willems, B., Kalogera, V., & Henninger, M. 2004, ApJ, 616, 414
Wu, J., Li, J., Zhang, J., et al. 2023, in Proc. of the 31st ACM International Conf. on Multimedia (New York: Association for Computing Machinery), 2477
Wu, Q. D., Wang, N., Yuan, J. P., et al. 2023a, ApJL, 958, L17
Wu, Q. D., Yuan, J. P., Wang, N., et al. 2023b, MNRAS, 522, 5152
Xie, M., Li, Y., Wang, Y., et al. 2022, in Proc. of the IEEE/CVF Conf. on Computer Vision and Pattern Recognition, 7993
Yao, J. M., Manchester, R. N., & Wang, N. 2017, ApJ, 835, 29